Hindawi
Advances in High Energy Physics
Volume 2021, Article ID 2489232, 13 pages
https://doi.org/10.1155/2021/2489232

Research Article

Strangeness Enhancement at LHC Energies Using the Thermal Model and EPOSLHC Event Generator

Mahmoud Hanafy,[1] **Omnia S. A. Qandil**,[2] **and Asmaa G. Shalaby**[1]

[1]*Physics Department, Faculty of Science, Benha University, Benha 13518, Egypt*
[2]*Mathematics and Theoretical Physics Department, Atomic Energy Authority, Cairo, Egypt*

Correspondence should be addressed to Mahmoud Hanafy; mahmoud.nasar@fsc.bu.edu.eg

Received 29 May 2021; Revised 6 November 2021; Accepted 26 November 2021; Published 16 December 2021

Academic Editor: Roelof Bijker

The strangeness enhancement signature of QGP formation at LHC energies is carefully tackled in the present study. Based on HRG, the particle ratios of mainly strange and multistrange particles are studied at energies from lower $\sqrt{s} \sim 0.001$ up to 13 TeV. The strangeness enhancement clearly appeared at more high energies, and the ratios are confronted to the available experimental data. The particle ratios are also studied using the Cosmic Ray Monte Carlo (CRMC) interface model with its two different event generators, namely, EPOS 1.99 and EPOSlhc, which show a good agreement with the model calculations at the whole range of the energy. We utilize them to produce some particles ratios. EPOS 1.99 is used to estimate particle ratios at lower energies from AGS up to the Relativistic Heavy Ion Collider (RHIC) while EPOSlhc is used at LHC energies. The production of kaons and lambda particles is studied in terms of the mean multiplicity in p-p collisions at energies ranging from 4 to 26 GeV. We find that both HRG model and the used event generators, EPOS 1.99 and EPOSlhc, can describe the particle ratios very well. Additionally, the freeze-out parameters are estimated for different collision systems, such as p-p and Pb-Pb, at LHC energies using both models.

1. Introduction

One of the most important signatures of the phase transition between the hadronic matter "confined phase" to the quark-gluon plasma (QGP) "deconfined phase" is the strangeness enhancement, in other words, the production of strange particles [1]. The abundance of "s" quark is a useful tool to analyze the heavy-ion and proton-proton collisions. Additionally, abundance of strangeness is considered as an abundance in the degree of freedom.

The strangeness enhancement is combined with gluon existence in QGP, in which the gluon dissolves to a pair of strange quarks rapidly [2]. An early study explored the phase transition from hadronic matter to QGP [3] and postulated the idea of chemical and thermal equilibrium which, in turn, developed the explanation of thermodynamics at high temperature and various kinds of chemical potentials.

It is noted that QGP comprises an equal number of strange and antistrange quarks [4]. Therefore, the density of strange quarks raises, and more multistrange hadrons are produced. This occurs during the hadronization process [5]. Recently, a good review [6] handled the strangeness production as a signature for QGP formation. The theoretical and experimental procedures are discussed besides tackling the nonstrange signature of QGP such as J/Ψ suppression.

In the present work, the hadron resonance gas (HRG) model is utilized as a powerful tool to analyze the production of hadrons resulting from various heavy-ion experiments such as AGS, SPS [7, 8], RHIC [9, 10], and LHC [11]. This is in addition to the previous work that investigated RHIC, LHC, and NICA energies [12, 13].

An earlier work [1] studied the strange and nonstrange production in the framework of excluded volume model which fits good with the experimental data. The strange to

nonstrange ratios are analyzed, in particular the kaon to pion and Λ to pion ratios in a canonical ensemble [14]. The results showed an effect of the system size, and as a consequence, the peak (horn) of such ratios is noticed at different energies. Another interesting work of the system-size dependence of hadrochemistry is applied [15]. There is an enhancement of multistrange hadrons in high-multiplicity pp collisions [16].

In addition, the particles $\phi(1020), K_s^{0*}(892)$ have a vital role in heavy-ion collisions [17] throughout the evolution process. This could be attributed to their short life times (4.16 ± 0.05 fm/c, 46.3 ± 0.4 fm/c), respectively, that facilitate analyzing the system at various times. The enhanced contribution of these particles is essential due to the strangeness enhancement.

The particle $\phi(1020), K_s^{0*}(892)$ production is studied [18] in lead-lead (Pb-Pb) and proton-proton (p-p) collisions at nucleon center of mass energy ($\sqrt{s_{\mathrm{NN}}}$=2.76 TeV). For a good knowledge, a pedagogic review in strangeness enhancement and papers therein is provided [19].

The main target of the present work is to investigate the strangeness enhancement in terms of various particle ratios such as k^+/π^+, k^-/π^-, π^-/π^+, k^-/k^+, $\bar{p}/\pi^-$, Λ/π^-, $\bar{\Lambda}/\Lambda$, $\bar{\Omega}/\Omega$, and $\bar{\Xi}^+/\Xi^-$ and strange and multistrange particles such as $\phi(1020)/k_s^{0*}(892)$, $\bar{\Sigma}^{*+8}/\Sigma^{*+8}$, $\bar{\Sigma}^{*08}/\Sigma^{*08}$, $\bar{\Sigma}^{*-8}/\Sigma^{*-8}$, $\bar{\Xi}^{*08}/\Xi^{*08}$, and $\bar{\Xi}^{*-8}/\Xi^{*-8}$ from low to high energies using different models, namely, HRG, EPOS 1.99, and EPOSlhc. Both event generators, EPOS 1.99 and EPOSlhc, are executed through the CRMC interface model to produce the above-mentioned particles for an ensemble of 100,000 events where the fusion option is turned on. The production of kaons and lambda particles is studied in terms of the mean multiplicity in p-p collisions at energies ranging from 4 to 26 GeV. First, we have used both event generators to produce well-identified particles and comparing the obtained results with the available experimental data. This encourages us to use it for a production of particles which have no experimental data. Also, the freeze-out parameters, i.e., the temperature (T_{ch}) and baryon chemical potential (μ_{B}), are estimated as a result of fitting the obtained results from the HRG model of a combination of the used particle ratios with both LHC and EPOSlhc results. The obtained values of T_{ch} and μ_{B} are compared to those presented in Ref. [20].

The present study is organized as follows: in Section 2, the main equations of the hadron gas model are discussed. A general introduction about the event generator is presented in Section 3. Section 4 presents the obtained results. Finally, the conclusion is represented in Section 5.

2. Formalism

In the present work, the grand canonical ensemble (GCE) is used in the framework of the HRG model. In GCE ensembles, the energy exchanges freely with the surrounding medium, so that the number of particles is no longer fixed. Such a system possess thermodynamic properties which can be obtained from the GCE partition function. The GCE has rigorous conserved quantum numbers such as the charge, strangeness, and baryon quantum numbers. Thus, the GCE partition function is defined as follows [21, 22]:

$$Z(T, V, \mu_Q) = Tr\left[\exp\left(-\beta\left(H - \sum_i \mu_{Q_i} Q_i\right)\right)\right], \quad (1)$$

where H is the Hamiltonian, Q_i is the different conserved charges, μ_{Q_i} are the corresponding chemical potentials, and $\beta = 1/T$ is natural units ($\hbar = c = k_B = 1$). The Hamiltonian in HRG includes all the degree of freedom. Then, the partition function in the hadron resonance gas can be written as a sum of partition functions of hadrons and resonances as follows [21, 22]:

$$\begin{aligned}\ln Z\left(T, V, \vec{\mu}\right) &= \sum_i \ln Z_i\left(T, V, \vec{\mu}\right) \\ &= \pm \sum_i \frac{V g_i}{(2\pi)^2} \int_0^\infty k^2 dk \ln\left[1 \pm \lambda_i \exp\left(-\beta \quad \varepsilon_i\right)\right],\end{aligned} \quad (2)$$

where the $\pm$ signs refer to fermions and bosons, respectively; $\varepsilon_i = \sqrt{k^2 + m_i^2}$ with m_i as the mass of "i" particle; and $\lambda_i(T, \vec{\mu})$ is the fugacity factor and is given by [21, 22]

$$\lambda_i\left(T, \vec{\mu}\right) = \exp\left(\frac{\mu_s S_i + \mu_q Q_i + \mu_B B_i}{T}\right), \quad (3)$$

where μ_s, μ_q, and μ_B are the strange, quark, and baryon chemical potentials, respectively, and S_i, Q_i, and B_i are the corresponding quantum numbers for particle species "i." These quantities should fulfill the conservation laws such as strangeness, $\sum_i S_i \quad N_i = 0$, and charge and baryon number, $\sum_i Q_i N_i / \sum_i B_i N_i = Z/A$, where Z and A are the atomic number and mass number of the colliding nuclei, respectively. The integration in equation (2) has been performed over "k" resulting in Bessel function K_2 [22].

$$\ln Z_i\left(T, V, \vec{\mu}\right) = \frac{VTg_i}{(2\pi)^2} \sum_{n=1}^{\infty} \frac{(\pm 1)^{n+1}}{n^2} \lambda_i^n m_i^2 K_2(n m_i \beta). \quad (4)$$

Therefore, the thermodynamic quantities can be obtained from equation(4). Then, the number density of particles is given by [22]

$$n_i\left(T, \vec{\mu}\right) = \frac{<N_i>}{V} = \frac{Tg_i}{(2\pi)^2} \sum_{n=1}^{\infty} \frac{(\pm 1)^{n+1}}{n^2} \lambda_i^n m_i^2 K_2(n m_i \beta). \quad (5)$$

where $<N_i>$ is the average number of the particles. In order to include all hadrons with their resonance decay, the average number can be rewritten as

$$<N_i>_{\mathrm{total}} = <N_i>^{\mathrm{th}} + \sum_j \mathrm{Br}(j \longrightarrow i) < N_j>^{\mathrm{th},R}. \quad (6)$$

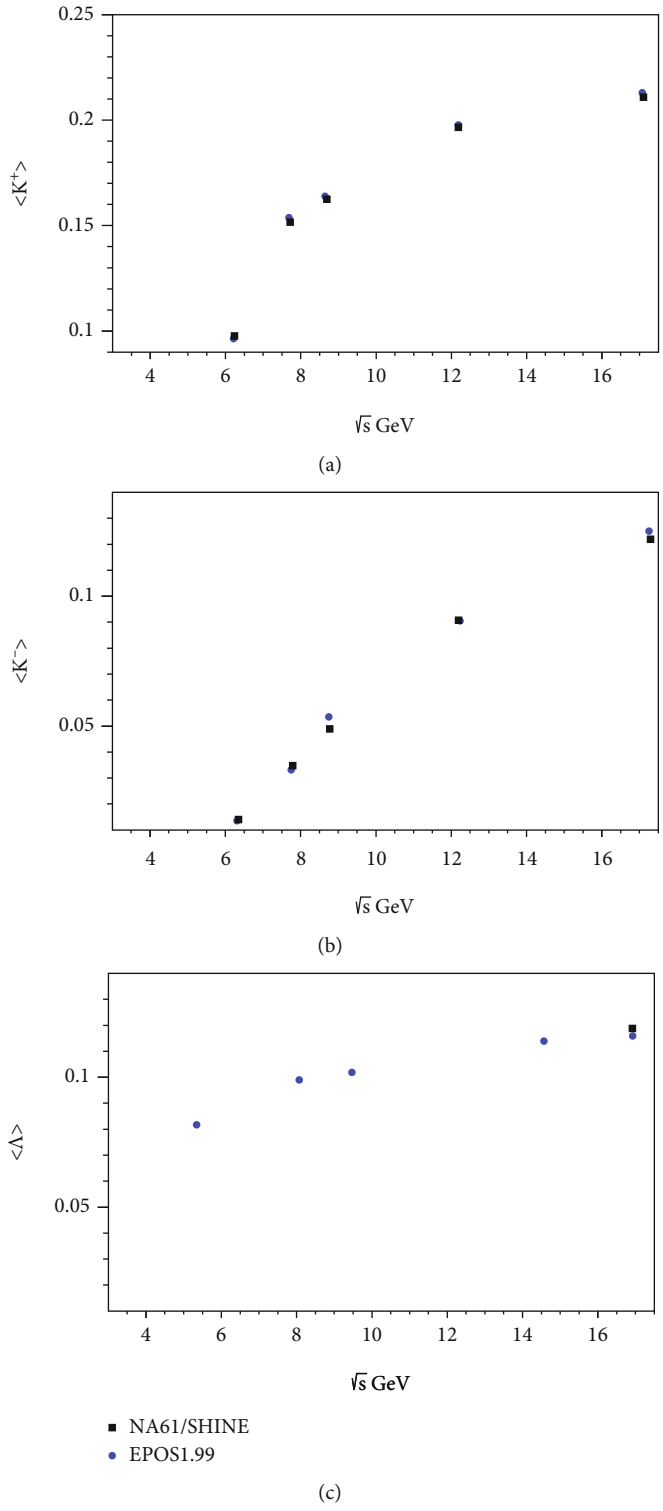

Figure 1: The mean multiplicity of the particles (a) k^+, (b) k^-, and (c) Λ generated from EPOS 1.99 in comparison with the experimental data taken from [33].

Table 1: The strange and multistrange particles with their quark structure and masses.

Particle	Quark content	Mass (GeV)
$\phi(1020)$	$s\bar{s}$	1.01946
$k_s^{0*}(892)$	$u\bar{s}$	0.89594
Λ	dus	1.11568
Ω	sss	1.67243
$\Xi\wedge-$	dss	1.32171
$\Sigma*^{+8}$	uus	1.3828
$\Sigma*^{08}$	dus	1.3837
$\Sigma*^{-8}$	dss	1.3872
Ξ^{*08}	uss	1.5318
Ξ^{*-8}	dss	1.535

where the first term represents the average number of thermal particles of species i and the second term represents all resonance contributions to the particle multiplicity of species i where "Br" stands for the branching ratio for the decay from particle ($j \longrightarrow i$). All particle ratios are calculated using equation (5).

3. Cosmic Ray Monte Carlo (CRMC)

CRMC is an interface which gives access to various Monte Carlo event generators such as EPOS 1.99, EPOSlhc, SIBYLL 2.1/2.3, and QGSJet 01/II.03/II.04 [23–25]. CRMC provides a full background description taking into account the produced diffraction. It is built on various types of interactions which are depending on the Gribov-Regee model such as EPOS 1.99 and EPOSlhc.

EPOS 1.99 and EPOSlhc are designed to explain both cosmic and noncosmic air showers and could be used to describe data produced from various collision systems such as proton-proton "p-p" or proton-nucleus "p-A" or deuteron-nucleus "d-Au" gold. Others in [23] presented a phenomenological approach based on the parton model trying to understand different experiments by a unified approach. They introduced EPOS, which stands for energy-conserving quantum mechanical multiple scattering approach, based on partons (parton ladders), off-shell remnants, and splitting of parton ladders [23]. EPOS is a sort of Monte-Carlo (MC) generator valid for heavy ion interactions and cosmic ray air shower simulations [24]. EPOS is confronted to Relativistic Heavy Ion Collider (RHIC) and Large Hadron Collider (LHC) data [23, 24].

Such (MC) models are essential to analyze the acceptance of the detector, the hadrons in the universe, and other impacted effect in astrophysics; all of them are confronted with high energy experiments [24]. In order to reproduce the LHC data [26–28] for p-p, p-Pb and Pb-Pb interactions, Pierog et al. [24] made the necessary modification in the model. There is another promising work [29] for the future analyzing the data from proton-oxygen (p-O) reaction at LHC energies. However, in the latter, they simulated the pseudorapidity spectra of charged pions, charged kaons, and protons at 13 TeV in p-p and p-O collisions at 10 TeV with CRMC.

In the present work, we utilize two different event generator EPOS 1.99 and EPOSlhc [30] at energies ranging from 0.001 up to 13 TeV for 100,000 events per energy to calculate the particle ratios k^+/π^+, k^-/π^-, π^-/π^+, k^-/k^+, $\bar{p}/\pi^-$, Λ/π^-, $\bar{\Lambda}/\Lambda$, $\bar{\Omega}/\Omega$, $\bar{\Xi}^+/\Xi^-$, and strange and multistrange particles such as $\phi(1020)/k_s^{0*}(892)$, $\bar{\Sigma}^{*+8}/\Sigma^{*+8}$, $\bar{\Sigma}^{*08}/\Sigma^{*08}$, $\bar{\Sigma}^{*-8}/\Sigma^{*-8}$, $\bar{\Xi}^{*08}/\Xi^{*08}$, and $\bar{\Xi}^{*-8}/\Xi^{*-8}$. EPOS 1.99 is performed at 7.7, 11.5, 19.6, 27, 39, 62.4, 130, and 200 GeV while EPOSlhc is executed at 0.9, 2.76, 5.02, 7, and 13 TeV for Pb-Pb collision. The resulting particle ratios are used to explain the strangeness enhancement signature.

4. Results and Discussion

In this section, the obtained results of different particle ratios using the HRG model are presented from $\sqrt{s} \sim 0.001$ up to $\sqrt{s} = 13$ TeV. All results are compared with the available experimental data. For some suggested strange and multistrange particles, there is a lack of experimental data; thus, we used two different generators, i.e., EPOS 1.99 and EPOSlhc, to predict their results. Also, the freeze-out parameters, i.e., T_{ch} and μ_{B}, are estimated as a result of fitting the obtained results from the HRG model of a combination of the calculated particle ratios with both LHC data and EPOSlhc event generator results for two different collisions systems, i.e., p-p and Pb-Pb, at $\sqrt{s} = 5.02$, 13 TeV, respectively. The obtained values of T_{ch} and μ_{B} are compared to the values presented in Ref. [20]. The calculated particle ratios as a function of various centers of mass energies are then used to explain the strangeness enhancement signature.

The first experimental data of strangeness enhancement in high-multiplicity pp collision is presented in [31] for strange and multistrange particles. These kick-off results motivated the authors of the current work to study the strange and multistrange particle enhancement. Additionally, they observed that there is a similarity in the strangeness production between p – p and Pb – Pb collisions for high-multiplicity events where the deconfined phase of matter (i.e., QGP) is formed. This conclusion is impacted again in different interesting works [20, 32]. The results are divided into three groups:

(i) Particle multiplicity versus the center of mass energy $\sqrt{s}$

Strangeness enhancement is considered as a signal of deconfinement in the ultrarelativistic heavy-ion collisions where there is an enhancement of the yields of hyperons relative to that of p-p nucleus collisions [33]. In this section, the EPOS 1.99 event generator is used to predict the mean multiplicities of the strange particles, k^+, k^-, and Λ, from p-p collisions at energies ranging from $\sqrt{s} = 4$ up to $\sqrt{s} = 26$ GeV in a rapidity range of $0 < y < 3$ as shown in Figure 1. The obtained results are confronted to those measured in NA61/SHINE experiment [33]. EPOS 1.99 event generator

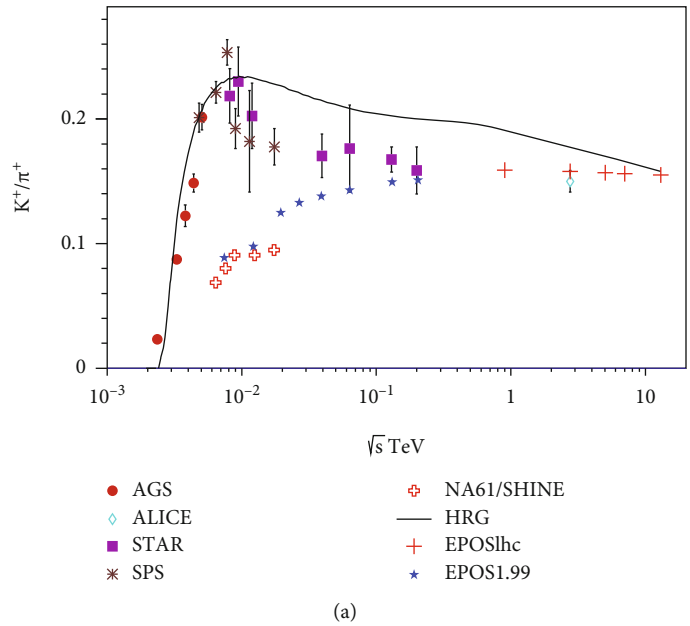

(a)

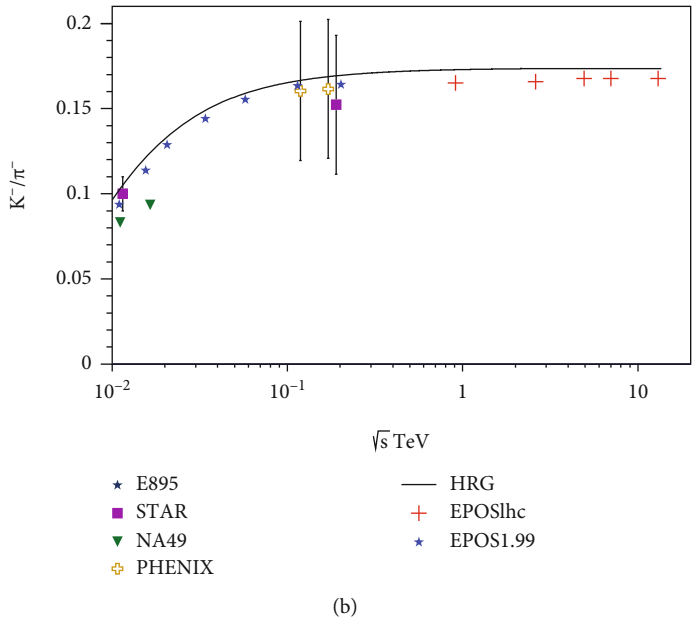

(b)

Figure 2: Continued.

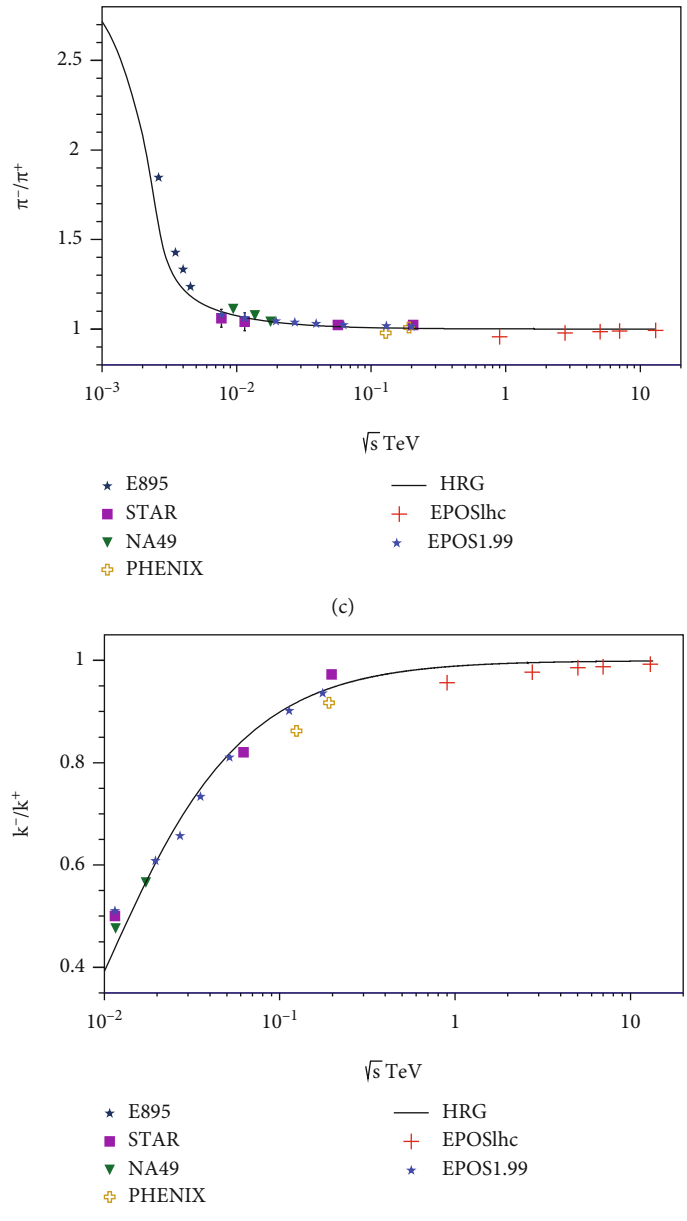

Figure 2: The energy dependence of the particle ratios k^+/π^+, k^-/π^-, π^-/π^+, and k^-/k^+ from the HRG model and EPOS 1.99 and EPOSlhc event generators in comparison with the experimental data taken from [36–38].

is succeeded very well to describe the multiplicity of k^+ as seen in Figure 1(a). In the case of k^-, there is a small deviation at $\sqrt{s} = 9$ and 19 GeV as shown in Figure 1(b). The multiplicity of Λ particle predicted by EPOS 1.99 event generator is shown in Figure 1(c) and has a good agreement with the experimental data taken from [33].

(ii) Particle ratios versus the center of mass energy $\sqrt{s}$

The particle ratios with the $\sqrt{s}$ including some heavier and strange particles are calculated by the HRG model and both event generators, i.e., EPOS 1.99 and EPOSlhc, at various energies spanning from $\sqrt{s} = 0.001$ up to $\sqrt{s} = 13$ TeV. The dependence of the baryon chemical potential and the temperature on the center of mass energy is taken from [34], which has an agreement with the parameterization in [35].

$$\mu_B = \frac{a}{1 + b\sqrt{s}}, \tag{7}$$

where $a = 1.245 \pm 0.094$ GeV and $b = 0.264 \pm 0.028$ GeV^{-1}. The temperature can also be defined in terms of the center of mass energy [34].

$$T = T_{\lim}\left[\frac{1}{1 + \exp\left(\left(1.172 - \log\left(\sqrt{S_{NN}}\right)\right)/0.45\right)}\right], \tag{8}$$

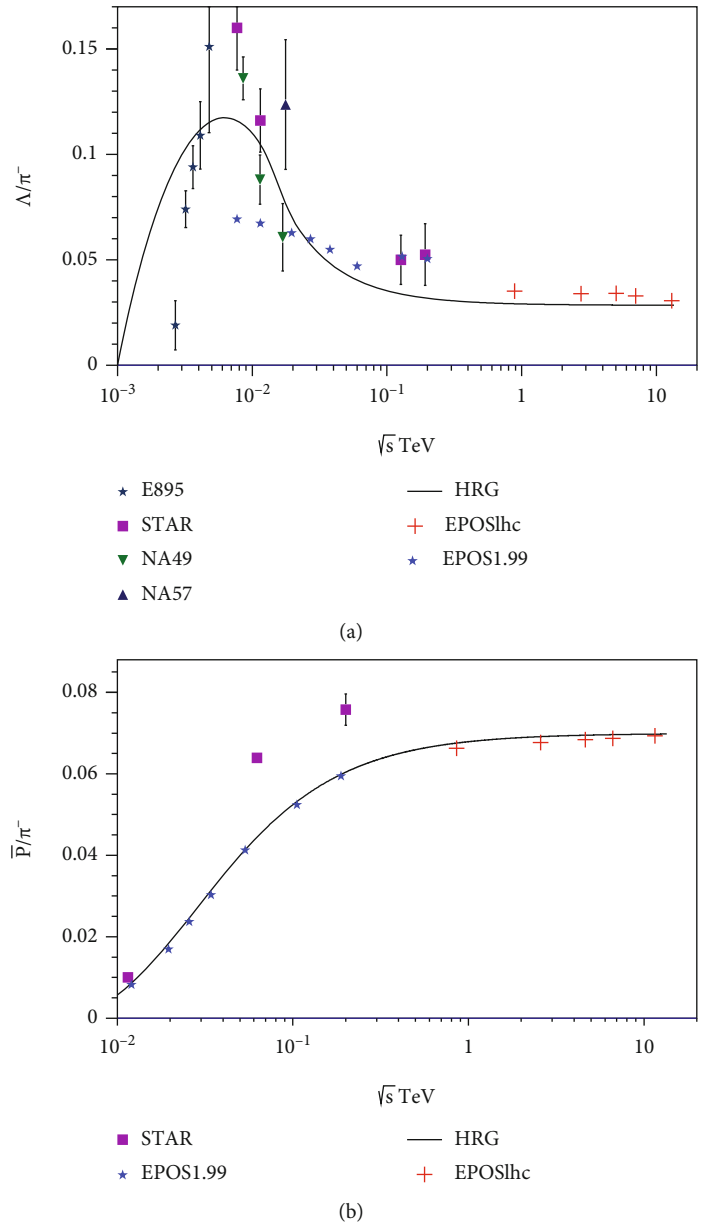

Figure 3: Continued.

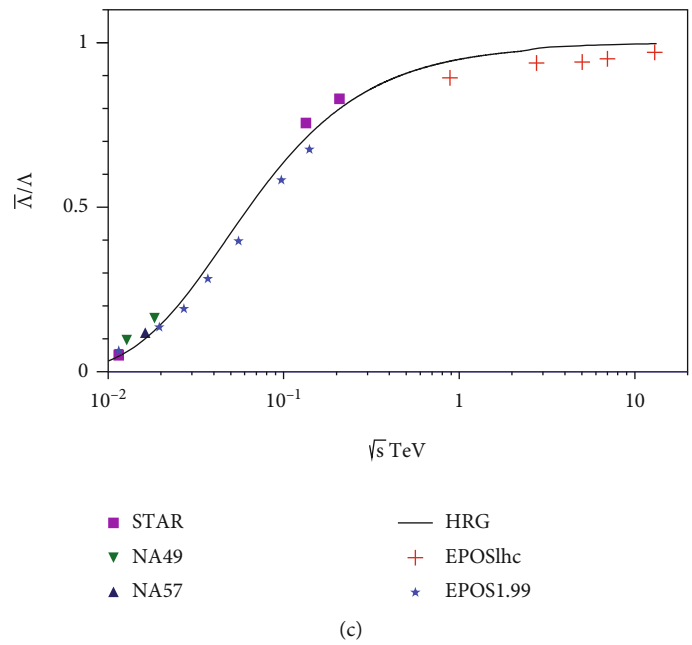

(c)

Figure 3: Similar to Figure 2, particle ratios Λ/π^-, $\bar{p}/\pi^-$, and $\bar{\Lambda}/\Lambda$, where the experimental data are taken from [36–44].

where $\sqrt{S_{NN}}$ is taken in GeV and $T_{lim} = 161 \pm 4$ MeV. The quark structure of the strange and multistrange particles suggested here is listed in Table 1.

The dependence of different particle ratios on $\sqrt{s}$ at LHC energies from GeV to TeV is studied utlizing the HRG model. Figure 2 illustrates the ratios of strange to nonstrange particles (upper panel) such as $K^+/\pi^+, K^-/\pi^-$ and pure nonstrange and strange ratios (lower panel) for $\pi^-/\pi^+, K^-/K^+$ versus the center of mass energy. These ratios are confronted to the experimental data [36–38], and EPOS 1.99 (used at low energies) and EPOSlhc (used at high energies) event generators from $10^{-3} \leq \sqrt{s} \leq 13$ TeV. Figure 2(a) shows the important particle ratio of K^+/π^+ which is used as characterising tool to describe the strangeness enhancement in the quantum chromodynamic (QCD) matter. This ratio shows a peak at $\sqrt{s} \simeq 9$ GeV which is known as the horn puzzle and might be considered as an indication of the QCD phase transition. The EPOS 1.99 event generator can describe the lowest NA61/SHINE data produced from p-p collisions at the center of mass energy $\sqrt{s} \simeq 7.5$ and 12.5 GeV and the highest STAR Pb-Pb collisions at $\sqrt{s} \simeq 200$ GeV while the EPOSlhc event generator can describe the ALICE data at $\sqrt{s} \simeq 3$ TeV. The wide range of energy shows the expected results in which there is a rapid enhancement in the strange particles only in the ratios $(K^-/\pi^-, K^-/K^+)$ as in Figures 2(b) and 2(d). However, Figure 2(a) shows a monotonic increasing (horn) up to $\sqrt{s} \sim 10$ GeV, then begin to decrease with increasing the energy, and a clear deceasing in the pure nonstrange particles with increasing the energy such as Figure 2(c).

Figure 3 presents the energy dependence of the particle ratios Λ/π^-, $\bar{p}/\pi^-$, and $\bar{\Lambda}/\Lambda$ in comparison with the experimental data taken from [36–38] and the estimated results from both EPOS 1.99 and EPOSlhc event generators. We notice that the horn puzzle appears again in the ratio Λ/π^- still at the range of GeV energy.

Figures 4 and 5 show a series of strange and multistrange particles such as $\bar{\Omega}/\Omega$, $\bar{\Xi}^+/\Xi^-$, ϕ/k_s^*, $\bar{\Sigma}^{*+8}/\Sigma^{*+8}$, $\bar{\Sigma}^{*08}/\Sigma^{*08}$, $\bar{\Sigma}^{*-8}/\Sigma^{*-8}$, $\bar{\Xi}^{*08}/\Xi^{*08}$, and $\bar{\Xi}^{*-8}/\Xi^{*-8}$ which are calculated in the framework of the HRG model and compared with the results obtained from both EPOS 1.99 and EPOSlhc event generators. It is clear that most of the strange and multistrange particles show strangeness enhancement as the energy increases up to 13 TeV. The $\phi(1020)/K_s^{0*}(892)$ [18] ratio shows a rapid enhancement at energies in GeV and smoothly increases at TeV. This ensures that the strangeness enhancement is a strong signature for the quark gluon plasma (QGP) creation at very high energy.

(iii) Fitting χ^2-tuning

Recently, fitting with particle ratios for both p – p and Pb – Pb collisions has been made in Ref. [32, 47]. They found that the HRG model fits very well and the grand canonical description is valid for the highest multiplicities. Figure 6 shows a fitting between the calculated particle ratios, i.e., particles shown in Table 2, from the HRG model using equation (5), and both LHC data [20] and EPOSlhc event generator results, using equation (9) in Pb – Pb and p – p collision systems at energies 5.02 and 13 TeV, respectively.

It is noticed that at 5.02 TeV for Pb – Pb collision, the theoretical results are rather matched with the experimental data compared to the fitted one in a previous study [20]. In the future work, we would focus on p-p collision [48] at LHC 7 TeV and high multiplicity and for Pb – Pb collisions at 2.76 TeV energies [49–52] due to its importance in the studying of the hadronic matter under extreme conditions.

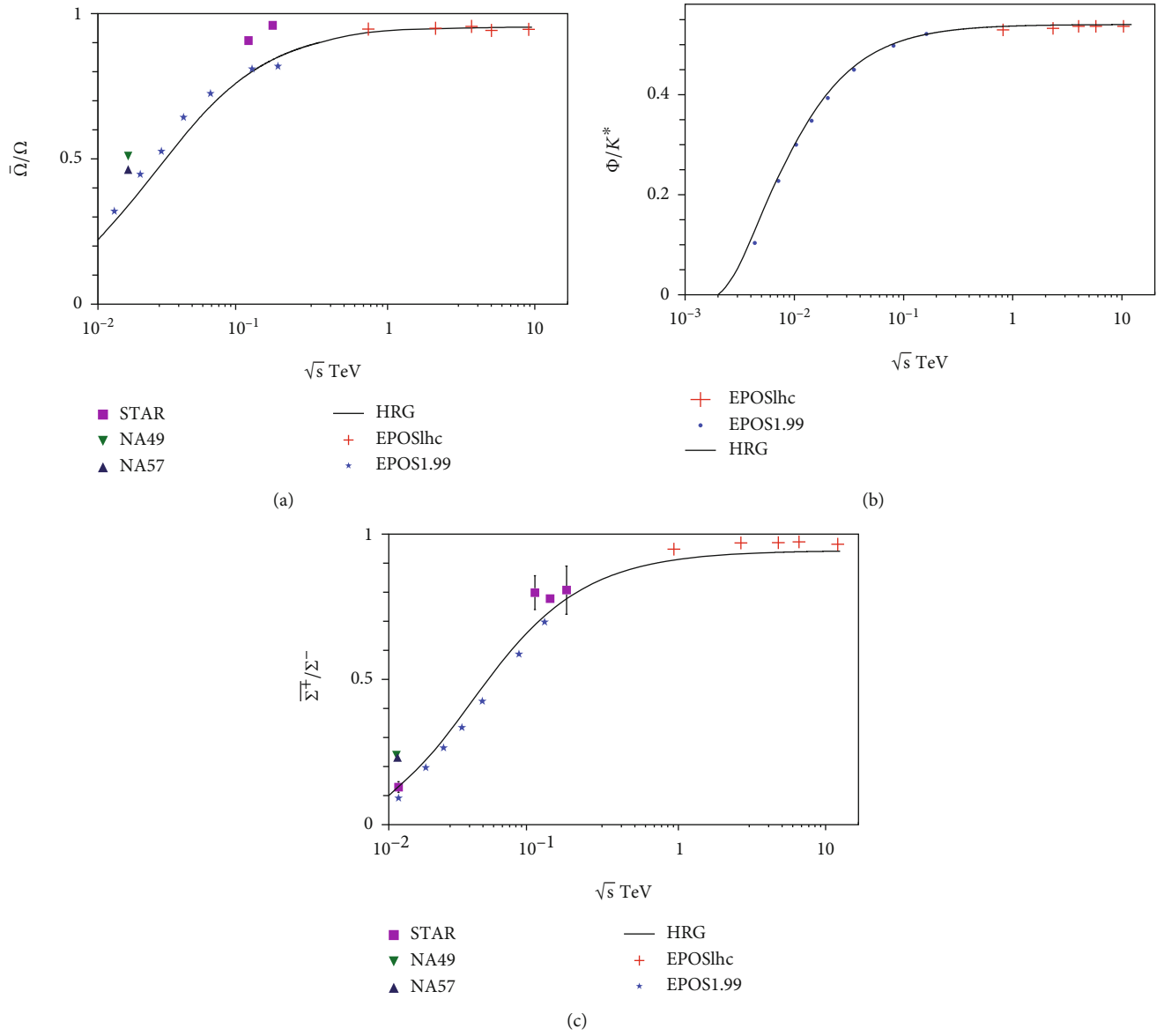

FIGURE 4: The same as in Figure 3, the particle ratios $\bar{\Omega}/\Omega$, $\bar{\Xi}^+/\Xi^-$, and ϕ/k_s^*, where the experimental data are taken from [44–46]. In the case of the particle ratio ϕ/k_s^*, no experimental data are available and both EPOS 1.99 and EPOSlhc are utilized for predictions.

The extracted chemical freeze-out temperature and baryon chemical potential are shown in Table 3. It seems that, hadronization occurs at 135 MeV and small μ_B 0.6 MeV as compared to a previous study [20] in which hadronization occurred at T_{ch} 140-160 MeV and $\chi^2/\text{do} = 48.529/3$ (dof: degree of freedom). However, in Ref. [20], the fitted particle ratios are 3 only; the present work is closer to the minimum fitted temperature $T_{ch} \sim 140$ MeV. On the other hand, the expected critical temperature in [53] is 156.5 ± 1.5 MeV.

(iv) Analysis of particle ratios

The statistical fit between the obtained results from the HRG model and both LHC data and EPOSlhc event generator are done as follows:

$$\chi^2 = \sum_i \frac{R_i^{\text{exp}} - R_i^{\text{model}}}{\sigma_i^2}, \tag{9}$$

where R_i^{exp} and R_i^{model} represent the experimental and computed values of the particle ratios, respectively. σ_i is the error in the experimental results.

In the present work, all hadrons and resonances are implemented from the particle data group (PDG) up to 11 GeV [17]. The main point in Table 3 is that the data agree fairly well with Pb-Pb collision but shows a great discrepancy for p-p collision. This note is marked in an earlier work [32], between the different system sizes and using the canonical and grand canonical ensemble, in which the latter was used in the present work.

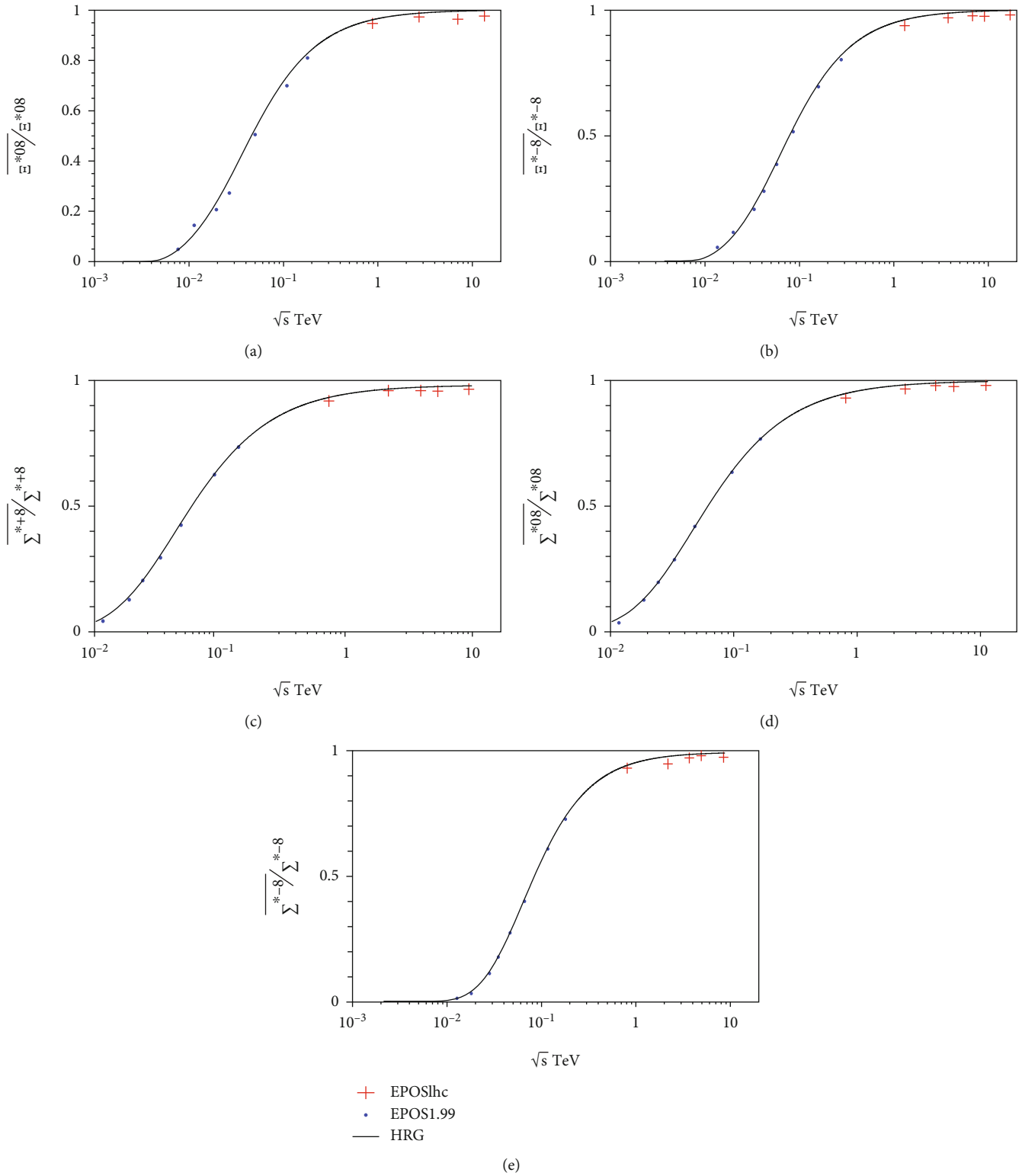

Figure 5: The same as in Figure 4 particle ratios $\bar{\Sigma}^{*+8}/\Sigma^{*+8}$, $\bar{\Sigma}^{*08}/\Sigma^{*08}$, $\bar{\Sigma}^{*-8}/\Sigma^{*-8}$, $\bar{\Xi}^{*08}/\Xi^{*08}$, and $\bar{\Xi}^{*-8}/\Xi^{*-8}$.

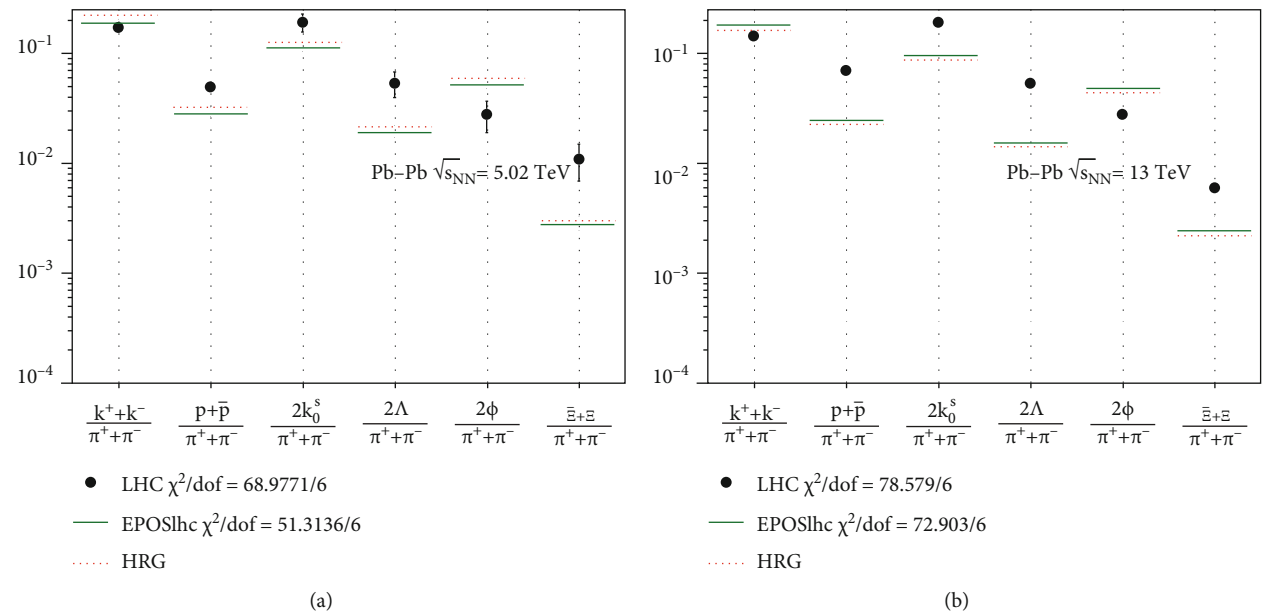

Figure 6: A statistical fit between the calculated particle ratios using the HRG model equation (5) and both LHC data [20] and EPOSlhc event generator results, using equation (9) in Pb – Pb and p – p collision systems at energies 5.02 and 13 TeV, respectively.

Table 2: A set of compound particle ratios used for fitting HRG model calculations with both LHC data [20] and EPOSlhc event generator in Pb – Pb and p – p collision systems at energies 5.02 and 13 TeV, respectively.

$\frac{k^+ + k^-}{\pi^+ + \pi^-}$	$\frac{p + \bar{p}}{\pi^+ + \pi^-}$	$\frac{2k_s^{0*}}{\pi^+ + \pi^-}$	$\frac{2\Lambda}{\pi^+ + \pi^-}$	$\frac{2\phi}{\pi^+ + \pi^-}$	$\frac{\Xi^+ + \Xi^-}{\pi^+ + \pi^-}$

Table 3: The estimated T_{ch} and μ_B as a result of fitting the calculated results from the HRG model of the particle ratios presented in Table 2 with both LHC and EPOSlhc results in comparison with those shown in [20].

$\sqrt{s}$ (TeV)	LHC			EPOSlhc			[20]		
	T_{ch} (GeV)	μ_B (MeV)	χ^2/dof	T_{ch} (GeV)	μ_B (MeV)	χ^2/dof	T_{ch} (GeV)	μ_B (MeV)	χ^2/dof
5.02	0.145 ± 0.0052	0.3 ± 0.0026	68.9771/6	0.140 ± 0.0043	0.35 ± 0.0031	51.3136/6	0.1491 ± 0.0021	—	48.529/3
13	0.149 ± 0.0042	0.25 ± 0.0025	78.579/6	0.147 ± 0.0032	0.27 ± 0.0028	72.903/6	0.1579 ± 0.0023	—	31.766/3

5. Conclusion

In the present work, various well-identified, strange, and multistrange particle ratios as a function of different centers of mass energies are studied using various models, namely, HRG model, EPOS 1.99, and EPOSlhc event generators. The aim of using both event generators is to predict the particle ratios that are not measured yet. The obtained results from both event generators and the HRG model are compared with the available experimental data and show a good agreement along the whole range of the considered $\sqrt{s}$. The strangeness enhancement is studied in terms of the strange particle multiplicities and the dependence of the center of mass energies of the mentioned particle ratios. The production of particles that contain one strange quark or multistrange quarks is enhanced. The ratio of strange particles is doubled from 0.5 to 1 at energies $\sqrt{s} = 0.001$ to 13 TeV; this is clearly shown in Figures 4 and 5. Such particles have no quarks in the colliding nuclei (Pb-Pb) or colliding nucleons (p-p). Therefore, the enhancement of these particles is considered a strong probe for the QGP formation. Particularly, the strange quarks may be produced from the deconfinement of matter phase. For more investigation of strangeness enhancement, EPOSlhc event generator is used alongside with the HRG model for strange, nonstrange, and multistrange particles; it is elaborated for Pb-Pb collision.

Fitting the HRG results with the experimental data has an important impact of using canonical and grand canonical ensemble, in which the latter has a global conservation of the different quantum numbers. The comparison of different ensembles has been carried out [32], and it was concluded that there are discrepancies between the different ensembles and with the various collision system sizes such as p – p, Pb – Pb, and p – Pb. This final conclusion motivates the authors to extend this work to study the different ensembles at LHC energies in TeV range.

Data Availability

Data supporting this systematic review or meta-analysis are from previously reported studies and datasets, which have been cited.

Conflicts of Interest

The authors declare that they have no conflicts of interest.

Acknowledgments

This paper has been assigned the permanent arXiv identifier 2105.14303.

References

[1] S. K. Tiwari and C. P. Singh, "Production of strange, non-strange particles and hypernuclei in an excluded-volume model," *Journal of Physics: Conference Series*, vol. 509, article 012097, 2014.

[2] P. Koch, B. Muller, and J. Rafelski, "From strangeness enhancement to quark–gluon plasma discovery," *International Journal of Modern Physics A*, vol. 32, no. 31, p. 1730024, 2017.

[3] J. Rafelski and R. Hagedorn, "From hadron gas to quark matter. 2," in *Statistical Mechanics of Quarks and Hadrons H. Satzed*, p. 253, North Holland Publ. Co., Amsterdam, North Holland, 1980.

[4] J. Rafelski, "Extreme states of nuclear matter," in *Proceedings of Workshop on Future Relativistic Heavy Ion Experiments*, p. 282, Darmstadt, Germany, 2015.

[5] M. Jacob and J. Tran Thanh van, "Quark matter formation and heavy ion collisions: a general review and status report," *Physics Reports*, vol. 88, no. 5, pp. 321–413, 1982.

[6] J. Rafelski, "Discovery of quark-gluon plasma: strangeness diaries," *The European Physical Journal Special Topics*, vol. 229, no. 1, article 90263, pp. 1–140, 2020.

[7] P. Braun-Munzinger, J. Stachel, J. P. Wessels, and N. Xu, "Thermal equilibration and expansion in nucleus-nucleus collision at the AGS," pp. 43–48, 1995, https://arxiv.org/abs/nucl-th/9410026.

[8] P. Braun-Munzinger, J. Stachel, J. P. Wessels, and N. Xu, "Thermal and hadrochemical equilibration in nucleus-nucleus collisions at the SPS," vol. B365, p. 1, 1996, https://arxiv.org/abs/nucl-th/9508020.

[9] W. Broniowski, W. Florkowski, and M. Michalec, "Thermal analysis of particle ratios and p_T spectra at RHIC," vol. B33, p. 761, 2002, https://arxiv.org/abs/nucl-th/0106009.

[10] W. Broniowski and W. Florkowski, "Strange particle production at RHIC in a single-freeze-out model," vol. C65, Article ID 064905, 2002https://arxiv.org/abs/nucl-th/0112043.

[11] P. Braun-Munzinger, "Physics of ultra-relativistic nuclear collisions with heavy beams at LHC energy," vol. A661, p. 261, 1999, https://arxiv.org/abs/nucl-ex/9908007.

[12] A. Tawfik, E. Gamal, and A. G. Shalaby, "Particle production at RHIC and LHC energies," *International Journal of Modern Physics*, vol. A30, p. 1550131, 2015.

[13] A. Tawfik, "Particle production and chemical freezeout from the hybrid UrQMD approach at NICA energies," *European Journal of Physics*, vol. 52, p. 324, 2016.

[14] H. Oeschler, J. Cleymans, B. Hippolyte, K. Redlich, and N. Sharma, "Collisions of small nuclei in the thermal model," vol. C77, p. 584, 2017, https://arxiv.org/abs/1609.03700.

[15] V. Vovchenko, B. Donigus, and H. Stoecker, "Canonical statistical model analysis of p-p, p-Pb, and Pb-Pb collisions at the LHC," vol. 100, Article ID 054906, 2019https://arxiv.org/abs/1906.03145.

[16] ALICE Collaboration, J. Adam, D. Adamová et al., "Enhanced production of multi-strange hadrons in high-multiplicity proton- proton collisions," *Nature Physics*, vol. 13, no. 6, pp. 535–539, 2017.

[17] K. A. Olive, K. Agashe, C. Amsler et al., "Review of particle physics," *Chinese physics C*, vol. 38, no. 9, article 090001, 2014.

[18] J. Adam, D. Adamová, M. M. Aggarwal et al., "$K^*(892)^0$ and $\phi(1020)$ meson production at high transverse momentum in pp and Pb-Pb collisions at $\sqrt{sNN} = 2.76$ TeV," vol. 95, Article ID 064606, 2017https://arxiv.org/abs/1702.00555.

[19] J. Rafelski, "Strangeness enhancement: challenges and successes," vol. 155, p. 139, 2008, https://arxiv.org/abs/0710.1931.

[20] R. Rath, A. Khuntia, and R. Sahoo, "System size and multiplicity dependence of chemical freeze-out parameters at the harge hadron collider energies," 2019, https://arxiv.org/abs/1905.07959.

[21] K. Redlich, J. Cleymans, H. Oeshlerd, and A. Tounsi, "Particle production and equilibration in heavy ion collisions," *Acta Physica Polonica*, vol. B33, p. 1609, 2002.

[22] P. Braun-Munzinger, K. Redlich, and J. Stachel, "Particle production in heavy ion collisions," 2004, https://arxiv.org/abs/nucl-th/0304013.

[23] K. Werner, F.-M. Liu, and T. Pierog, "Parton ladder splitting and the rapidity dependence of transverse momentum spectra in deuteron-gold collisions at the BNL relativistic heavy ion collider," *Physics Review*, vol. C74, article 044902, 2006.

[24] T. Pierog, I. Karpenko, J. M. Katzy, E. Yatsenko, and K. Werner, "EPOS LHC : test of collective hadronization with LHC data," vol. 92, Article ID 034906, 2015https://arxiv.org/abs/1306.0121.

[25] https://web.ikp.kit.edu/rulrich/crmc.html.

[26] CMS collaboration, "Study of the inclusive production of charged pions, kaons, and protons in pp collisions at sqrt(s) = 0.9, 2.76, and 7 TeV," vol. 72, no. 2164, 2012https://arxiv.org/abs/1207.4724.

[27] K. Aamodt, N. Abel, U. Abeysekara et al., "Charged-particle multiplicity measurement in proton–proton collisions at $\sqrt{s}$ = 7 TeV with ALICE at LHC," vol. 68, no. 345, 2010https://arxiv.org/abs/1004.3514.

[28] Atlas Collaboration, "Charged-particle multiplicities in pp interactions measured with the ATLAS detector at the LHC," vol. 13, Article ID 053033, 2011https://arxiv.org/abs/1012.5104.

[29] H. P. Dembinski, R. Ulrich, and T. Pierog, "PoS(ICRC2019)235," in *36th International Cosmic Ray Conference*, Madison WI U.S.A, 2019.

[30] M. Hanafy, A. Tawfik, M. Maher, and W. Scheinast, "Particle ratios within EPOS, UrQMD and thermal models at AGS, SPS and RHIC energies," 2021, https://arxiv.org/abs/1907.05729.

[31] J. Adam and ALICE Collaboration, "Enhanced production of multi-strange hadrons in high-multiplicity proton–proton collisions," *Nature Physics*, vol. 13, no. 535, 2017.

[32] N. Sharma, J. Cleymans, B. Hippolyte, and M. Paradza, "A comparison of p-p, p-Pb, Pb-Pb collisions in the thermal model: multiplicity dependence of thermal parameters," vol. 99, Article ID 044914, 2019https://arxiv.org/abs/1811.00399.

[33] A. Aduszkiewicz et al., *The European Physical Journal C*, vol. 77, no. 671, 2017.

[34] A. Tawfik and E. Abbas, "Thermal description of particle production in Au-Au collisions at STAR energies," vol. 12, no. 521, 2015https://arxiv.org/abs/1311.7508.

[35] J. Cleymans, H. Oeschler, K. Redlich, and S. Wheaton, "Comparison of chemical freeze-out criteria in heavy-ion collisions," *Physics Review*, vol. C73, article 034905, 2006.

[36] J. Adams, C. Adler, M. M. Aggarwal et al., "Identified particle distributions in *pp* and Au+Au collisions at $\sqrt{s_{NN}} = 200$ GeV," vol. 92, Article ID 112301, 2004https://arxiv.org/abs/nucl-ex/0310004.

[37] S. V. Afanasiev, T. Anticic, D. Barna et al., "Energy dependence of pion and kaon production in central Pb+Pb collisions," vol. 66, Article ID 054902, 2002https://arxiv.org/abs/nucl-ex/0205002.

[38] C. Alt, T. Anticic, B. Baatar et al., "Pion and kaon production in central Pb+Pb collisions at 20A and 30A GeV: evidence for the onset of deconfinement," vol. 77, Article ID 024903, 2008https://arxiv.org/abs/0710.0118.

[39] T. Anticic, B. Baatar, D. Barna et al., "Λ and $\bar{\Lambda}$ production in central Pb-Pb collisions at 40, 80, and 158 A·GeV," vol. 93, Article ID 022302, 2004https://arxiv.org/abs/nucl-ex/0311024.

[40] NA49 Collaboration, "Energy dependence of Lambda and Xi production in central Pb+Pb collisions at 20A, 30A, 40A, 80A, and 158A GeV measured at the CERN Super Proton Synchrotron," vol. 78, Article ID 034918, 2008https://arxiv.org/abs/0804.3770.

[41] C. Pinkenburg and for the E895 Collaboration, "Production and collective behavior of strange particles in Au + Au collisions at 2–8 AGeV," 2002, https://arxiv.org/abs/nucl-ex/0104025.

[42] C. Alt and NA49 collaboration, "Omega and antiomega production in central Pb+Pb collisions at 40 and 158 AGeV," vol. 94, Article ID 192301, 2005https://arxiv.org/abs/nucl-ex/0409004.

[43] L. Ruan and S.T.A.R. Collaboration, "π, K, p and production from Au+ Au collisions at 62.4 GeV," *Journal of Physics G: Nuclear and Particle Physics*, vol. 31, no. 6, article S1029, p. S1033, 2005.

[44] S. V. Afanasiev and NA49 Collaboration, "Cascade and anticascade production in central Pb+Pb collisions at 158 GeV/c per nucleon," vol. 538, no. 275, 2002https://arxiv.org/abs/hep-ex/0202037.

[45] F. Antinori, P. A. Bacon, A. Badala et al., "Energy dependence of hyperon production in nucleus-nucleus collisions at SPS," *Physics Letters B*, vol. 595, no. 1, pp. 68–74, 2004.

[46] M. M. Aggarwal, Z. Ahammed, A. V. Alakhverdyants et al., "Strange and multi-strange particle production in Au+Au collisions at $\sqrt{s_{NN}} = 62.4\,GeV$," vol. 83, Article ID 024901, 2011https://arxiv.org/abs/1010.0142.

[47] N. Sharma, J. Cleymans, and L. Kumar, "Thermal model description of p–Pb collisions at $\sqrt{s_{NN}} = 5.02\,TeV$," *The European Physical Journal C*, vol. 78, no. 288, 2018.

[48] A. Khuntia, H. Sharma, S. K. Tiwari, R. Sahoo, and J. Cleymans, "Strangeness enhancement at LHC energies using the thermal model and EPOSLHC event-generator," vol. A55, p. 3, 2019, https://arxiv.org/pdf/2105.14303.pdf.

[49] J. Adam, D. Adamova, M. M. Aggarwal et al., "Centrality dependence of the charged-particle multiplicity density at mid-rapidity in Pb-Pb collisions at $\sqrt{s_{NN}} = 5.02$ TeV," vol. 116, Article ID 222302, 2016https://arxiv.org/abs/1512.06104.

[50] K. Aamodt and ALICE Collaboration, "Centrality dependence of the charged-particle multiplicity density at mid-rapidity in Pb-Pb collisions at $\sqrt{s_{NN}} = 2.76$ TeV," vol. 106, Article ID 032301, 2011https://arxiv.org/abs/1012.1657.

[51] G. Aad and ATLAS collaboration, "Measurement of the pseudorapidity and transverse momentum dependence of the elliptic flow of charged particles in lead-lead collisions at $\sqrt{s_{NN}} = 2.76$ TeV with the ATLAS detector," vol. 710, no. 363, 2012https://arxiv.org/abs/1108.6018.

[52] S. Chatrchyan, V. Khachatryan, A. M. Sirunyan et al., "Dependence on pseudorapidity and centrality of charged hadron production in PbPb collisions at a nucleon-nucleon centre-of-mass energy of $\sqrt{s_{NN}} = 2.76$ TeV," vol. 8, no. 141, 2011https://arxiv.org/abs/1107.4800.

[53] A. Bazavov, H. T. Ding, P. Hegde et al., "Chiral crossover in QCD at zero and non-zero chemical potentials," vol. B795, p. 15, 2019, https://arxiv.org/abs/1812.08235.